

AD/A-000 930

STABILIZED LASER GRAVIMETER

Howard C. Merchant

Washington University

Prepared for:

Air Force Cambridge Research Laboratories

22 July 1974

DISTRIBUTED BY:

NTIS

National Technical Information Service
U. S. DEPARTMENT OF COMMERCE
5285 Port Royal Road, Springfield Va. 22151

Unclassified

Security Classification

AD/A-000930

DOCUMENT CONTROL DATA - R&D		
<i>(Security classification of title, body of abstract and indexing annotation must be entered when the overall report is classified)</i>		
1. ORIGINATING ACTIVITY (Corporate author) University of Washington Applied Physics Laboratory Seattle, Washington 98195		2a. REPORT SECURITY CLASSIFICATION Unclassified 2b. GROUP
2. REPORT TITLE STABILIZED LASER GRAVIMETER		
4. DESCRIPTIVE NOTES (Type of report and inclusive dates) SCIENTIFIC FINAL 1 May 1974 - 31 Jun. 1974		
3. AUTHOR(S) (First name, middle initial, last name) Howard C. Merchant		
6. REPORT DATE 22 July 1974	7a. TOTAL NO. OF PAGES 38	7b. NO. OF REFS 19
8a. CONTRACT OR GRANT NO. F19628-73-C-0203	9a. ORIGINATOR'S REPORT NUMBER(S) APL-UW 7419	
8b. PROJECT, TASK, WORK UNIT NOS. 7600-06-01	9b. OTHER REPORT NO(S) (Any other numbers that may be assigned this report) AFCRL-TR-74-0355	
8c. DOD ELEMENT 62101F		
8d. DOD SUBELEMENT 587600		
10. DISTRIBUTION STATEMENT Approved for public release: Distribution unlimited.		
11. SUPPLEMENTARY NOTES Tech. Other	12. SPONSORING MILITARY ACTIVITY Air Force Cambridge Research Laboratories (LWG) Hanscom AFB, Mass. 01730 Contract Monitor: James A. Hammond/LWG	
13. ABSTRACT The design, development and testing of a stabilized laser gravimeter are described. In this design a mirror forming one end of a Fabry-Perot optical cavity is mounted on a unique mechanical suspension system using endloaded beams. The low frequency suspension required for high sensitivity is obtained by making use of the decrease in frequency of a vibrating beam system with increasing end load. The wavelength of an external HeNe illuminating laser is tuned to maximize the output of the Fabry-Perot cavity by following a fringe. The reference length for the system is provided by a second laser whose wavelength is stabilized by a vibration-rotation absorption line in methane. The output of the system is the beat frequency between the two lasers. The sensitivities of the optical and mechanical systems have been demonstrated separately in laboratory tests. Further testing will involve the measurement of earth tides in the field.		

DD FORM 1473
NOV 61

UNCLASSIFIED
INFORMATION

Unclassified
Security Classification

Unclassified
Security Classification

14. KEY WORDS	LINK A		LINK B		LINK C	
	ROLE	WT	ROLE	WT	ROLE	WT
Laser						
Gravimeter						
Gravity						
Geophysical Instrumentation						

Unclassified
Security Classification

ia

CONTENTS

ACKNOWLEDGMENTS.....	v
RELATED DOCUMENTS AND PUBLICATIONS	vi
INTRODUCTION.....	1
TECHNICAL CONSIDERATIONS.....	2
Electro-optical System.....	2
Mechanical System.....	5
SYSTEM DESIGN.....	11
Electro-optical.....	11
Mechanical.....	12
SYSTEM OPERATION.....	14
Optical Alignment.....	14
Mechanical Alignment.....	14
Data Acquisition.....	15
RESULTS.....	15
Mechanical System.....	15
Electro-optical System.....	16
Overall System Performance.....	16
CONCLUSIONS AND RECOMMENDATIONS.....	17
REFERENCES.....	29

LIST OF FIGURES

Figure

- 1 Cavity-laser system
- 2 Transmission characteristics of a Fabry-Perot etalon
- 3 Retro-reflector suspension
- 4 Gravitational compensation
- 5 Retro-reflector subassembly
- 6 Assembled Fabry-Perot cavity
- 7 Upper mirror assembly
- 8 System schematic
- 9 Frequency vs end load
- 10 Asymmetry of the methane line
- 11 Structural stiffener
- 12 Ground motion record

ACKNOWLEDGMENTS

The following people contributed to the development of the system described here and/or to the text of this report:

Dr. E. Rodney Huggett

Dr. E. Norman Hernandez

Mr. Norman D. McMullen

Mr. Emil F. Homuth

Mr. Karlheinz Eisenger

The many helpful discussions with Prof. Stewart W. Smith and Dr. James A. Hammond are also acknowledged. A special acknowledgment is also in order for the effort put forth by Mr. Norman McMullen whose Master Thesis was based on this work.

RELATED DOCUMENTS AND PUBLICATIONS

The following quarterly reports were made on this contract (F19628-73-C-0203):

Laser Stabilized Gravimeter #1
(May 1, 1973 to July 31, 1973)

Laser Stabilized Gravimeter #2
(August 1, 1973 to October 31, 1973)

Laser Stabilized Gravimeter #3
(November 1, 1973 to January 31, 1974)

Laser Stabilized Gravimeter #4
(February 1, 1974 to April 30, 1974)

H.C. Merchant, E.N. Hernandez, and N.D. McMullen, "Stabilized Laser Gravimeter," Proceedings of the 20th International Instrumentations Symposium, Albuquerque, New Mexico, May 1974.

N.D. McMullen, "Methane Absorption Stabilized Laser Gravimeter: Design of an Ultra-Sensitive Fabry-Perot Interferometer Accelerometer," M.S. Thesis, Mechanical Engineering, University of Washington, 1974.

INTRODUCTION

The instrument described here is a portable static gravimeter as opposed to a pendulum or free-fall apparatus.

The static gravimeter consists of a mass elastically suspended so that changes in gravitation (or acceleration) will result in a detectable relative motion of the seismic mass. In the present design the mass consists of a mirror and holder, and the detection system uses two lasers. The mirror is the retro-reflector of a high-finesse Fabry-Perot cavity, an optical resonator with very narrow transmission fringes. The wavelength of an external HeNe illuminating laser is locked to changes in the cavity length by following a single fringe. The reference length is provided by a second HeNe laser which is stabilized by inserting a methane cell in the cavity, and locking the laser frequency to the molecular absorption line of methane. The output is the beat frequency between the stabilized reference laser and the cavity-locked laser. The optical system is an adaptation of the techniques used by Levine and Hall [1] for a strainmeter.

The microgal resolution required for a useful gravimeter requires a very high resolution laser and a very low natural frequency (soft) mechanical suspension system. To obtain the necessary mechanical sensitivity, a novel suspension system consisting of endloaded beams was used. Theoretically the natural frequency and spring stiffness of the system approach zero and infinity, respectively, as the end load approaches the buckling load for the beam system [2-1]. The system is compact and portable, unwanted modes can be controlled, and the operating characteristics can be easily changed even under field conditions.

-
1. J. Levine and J.L. Hall, "Design and Operation of a Methane Absorption Stabilized Laser Strainmeter," Journal of Geophysical Research, Vol. 77, No. 14 (May 1972) pp. 2595-2609.
 2. L. Meirovitch, Analytical Methods in Vibrations, Macmillan, New York (1967).
 3. D. Burgreen, "Free Vibrations of a Pin-Ended Column with Constant Distance Between Pin Ends," Journal of Applied Mechanics, June 1951, pp. 135-139.
 4. H. Lurie, "Lateral Vibrations as Related to Structural Stability," Journal of Applied Physics, June 1952, pp. 195-204.

TECHNICAL CONSIDERATIONS

Electro-optical System

The electro-optical system used for measuring the seismic mass deflections is essentially the same as the system used by Levine and Hall [1]. The system uses a Fabry-Perot cavity, whose retro-reflector is the seismic mass, and dynamically adjusts the frequency of the illuminating laser (3.39 μ HeNe) to follow a single fringe. The reference length is provided by a second 3.39 μ HeNe laser whose wavelength is stabilized by locking on to the vibration-rotation absorption line in methane with a first derivative feedback servosystem.

A quantitative analysis of the frequency stability of this laser is extremely complicated, but a simple physical model analogous to the model of the Lamb dip [5,6] contains the essential ideas. The helium-neon cell can provide gain over a relatively wide range of frequencies given by the Doppler width of the neon line. This width is of the order of 360 MHz. The laser can be forced to operate on a single frequency by properly constructing the cavity so that only one sufficiently high-Q mode lies within the Doppler profile. A standing wave, which can be thought of as two traveling waves moving in opposite directions, will be set up in the cavity. If the frequency of oscillation does not correspond to the methane absorption frequency, only methane molecules whose velocity down the cell axis is high enough to provide the requisite Doppler shift will absorb the radiation. The two running waves will be absorbed by two different velocity groups. This absorption will cause two "holes" to appear in the velocity distribution of methane molecules in the state that absorbed the energy. As the oscillation frequency is brought closer and closer to the methane line center, methane molecules with smaller and smaller Doppler shifts are excited until, at the center of the methane line, only molecules with no Doppler shift are excited. At this point, both running-wave fields will be absorbed by molecules that have zero velocity along the laser axis. This resulting extra depletion of methane molecules reduces the intracavity absorption at molecular line center, and therefore results in increased laser output power at this frequency.

Seismic mass deflections are interpreted as changes in the long path laser frequency. The long path laser (illuminating laser) consists of a non-confocal mirror system, i.e., the mirrors do not have a common center of curvature. One mirror is fixed permanently and the other mirror is mounted on a piezoelectric element. By illuminating the Fabry-Perot cavity with the long path laser, dithering the piezoelectric element through known deflections (determined empirically for optimum servosystem error and stability), and detecting the intensity of light transmitted, an error signal is generated which makes it possible to lock on to a single fringe using a first derivative feedback servosystem.

-
5. W.R. Bennett, Jr., "Hole Burning Effects in a HeNe Optical Laser," Physics Review, Vol. 126 (1962) p. 580.
 6. W.R. Bennett, Jr., "Hole Burning Effects in Gas Lasers with Saturable Absorbers," Comments on Atomic Molecular Physics, Vol. 2 (1970) p. 10.

The Fabry-Perot cavity is a half concentric mirror system (Figure 1). The hemispherical mirror is rigidly fixed, and the flat mirror is mounted in the seismic mass. For a Fabry-Perot cavity varying about length, L , the change in transmission frequency, Δf , corresponding to a change in cavity length, ΔL , is given by

$$\frac{\Delta f}{f} = -\frac{\Delta L}{L} \quad (1)$$

where f is the frequency of the monochromatic light.

In order to continuously follow the fringes of the Fabry-Perot cavity, it is important that the free spectral range of the cavity be less than that of the long path laser. This is required so that no transmission fringes will exist outside the monotonic frequency range of the illuminating laser. The free spectral range of a Fabry-Perot cavity is given by

$$\Delta f_r = \frac{C}{2L}, \quad (2)$$

where C is the velocity of light (3×10^8 m/sec), and L is the separation of the mirrors.

Since the resolution of the system depends on how accurately a fringe is followed, it is necessary to know the width of a single fringe, which is given by

$$\text{FWHM} = \frac{\Delta f_r}{F}, \quad (3)$$

where FWHM is the full width at half maximum, Δf_r is the free spectral range, and F is the finesse of the cavity. The finesse of a Fabry-Perot cavity, Figure 2, is given by [7]

$$F = \frac{(\pi/2)}{\sin^{-1}[(1-R)/2(R)^{1/2}]}, \quad (4)$$

where R is the reflectivity of the mirrors. For large values of R ,

$$F \approx \frac{\pi R^{1/2}}{(1-R)}. \quad (5)$$

The sensitivity of the system for a given FWHM is then determined as the fraction of FWHM needed in order to operate the servosystem above noise levels.

7. A. Yariv, Introduction to Optical Electronics, Holt, Rinehart and Winston, New York (1971).

Another important set of parameters is the spot size on the two reflectors within the Fabry-Perot cavity, and the extent to which the cavity can be mode matched with the illuminating laser. The intracavity spot sizes are important in the selection of mirror diameters since all light must be contained by the reflectors. Suitable mode matching optics produce near-perfect single-mode illumination of the Fabry-Perot cavity, which is essential if the full sensitivity of the instrument is to be realized [1,8].

In order to mode match the illuminating laser with the Fabry-Perot cavity, it is necessary to transform the properties of the Gaussian beam emitted by the laser to the properties of the resonator. This can be accomplished by lenses or mirrors. By knowing the locations and diameters of the beam waists of the beams to be transformed, one can locate the matching device of focal length f , where $f > f_0$, by the relations [8,9]

$$d_1 = f \pm \frac{W_1}{W_2} (f^2 - f_0^2)^{1/2}, \quad (6)$$

$$d_2 = f \pm \frac{W_2}{W_1} (f^2 - f_0^2)^{1/2}, \quad (7)$$

where

$$f_0 = \pi W_1 W_2 / \lambda \quad (8)$$

and the remaining parameters are defined in Figure 1.

The output of the system is obtained by mixing the beams from the two laser systems and monitoring the heterodyne frequency. The change in heterodyne frequency is proportional to the change in the Fabry-Perot cavity resonance and hence to the deflection of the seismic mass carrying the mirror.

8. H. Kogelnik and T. Li, "Laser Beams and Resonators," Applied Optics, Vol. 5, No. 10 (October 1966) pp. 1550-1567.

9. N.D. McMullen, "Methane Absorption Stabilized Laser Gravimeter: Design of an Ultra-Sensitive Fabry-Perot Interferometer Accelerometer," M.S. Thesis, Mechanical Engineering, University of Washington, 1974.

Mechanical System

The general equation for a beam with a concentrated mass and end loading, taking rotatory inertia and shear into account, but neglecting damping, is [2, 10-12]

$$EI \frac{\partial^4 y}{\partial x^4} + \mu \frac{\partial^2 y}{\partial x^2} - \left(\frac{\mu I}{A} + \frac{EI\mu}{AK'G} \right) \frac{\partial^4 y}{\partial x^2 \partial t^2} + \frac{\mu^2 I}{AK'G} \frac{\partial^4 y}{\partial t^4} + \frac{\partial}{\partial x} \left(P \frac{\partial y}{\partial x} \right) = 0 \quad (9)$$

If the geometric nonlinearity due to a fixed endload is taken into account [3],

$$P(x) = P_0 - \frac{\Lambda E}{2L} \int_0^L \left(\frac{\partial y}{\partial x} \right)^2 dx \quad (10)$$

The last term in Eq. 9 then becomes

$$\frac{\partial}{\partial x} \left[P(x) \frac{\partial y}{\partial x} \right] = P_0 \frac{\partial^2 y}{\partial x^2} - \frac{\Lambda E}{2L} \frac{\partial^2 y}{\partial x^2} \int \left(\frac{\partial y}{\partial x} \right)^2 dx \quad (11)$$

where the boundary conditions are

$$y(0,t) = 0 \quad (12)$$

$$\frac{\partial y}{\partial x}(0,t) = 0 \quad (13)$$

$$\frac{\partial y}{\partial x}(L,t) = 0 \quad (14)$$

$$EI \frac{\partial^3 y}{\partial x^3}(L,t) - \left(\frac{\mu I}{A} + \frac{EI\mu}{AK'G} \right) \frac{\partial^3 y}{\partial x \partial t^2}(L,t) - m \frac{\partial^2 y}{\partial t^2}(L,t) = 0 \quad (15)$$

where

E = Modulus of elasticity

I = Area moment of inertia

-
10. M.A. Southwell, Translated from Russian by M.G. Yatsua, "On the Correction for Shear of the Differential Equation for Transverse Vibrations of Prismatic Bars," Philosophical Magazine, Vol. 41 (May 1921) pp. 288-290.
 11. J.C. Snowdon, "Transverse Vibration of Beams with Internal Damping, Rotary Inertia, and Shear," Journal of the Acoustical Society of America, Vol. 35, No. 12 (December 1963) pp. 1997-2006.
 12. S. Timoshenko, Vibration Problems in Engineering, VanNostrand, New York (1955).

μ = Mass per unit length
 A = Cross sectional area of continuous beam
 K' = Shape factor
 G = Shear modulus
 m = One-half mass of seismic mass
 P = End load
 P_0 = Constant end preload
 L = Length of continuous member
 t = Time,

and the other variables are defined in Figure 3.

It is quite possible to solve Eq. 9 by finite element methods using a digital computer [13], but the level of accuracy required for the frequency predictions and responses makes this unnecessary. It should also be noted that this model does not include asymmetric modes of vibration. Detailed consideration of asymmetric modes is not necessary since their excitation is unlikely (e.g., tilting of the earth's surface is small at low frequencies), and, even if such an excitation did occur, it would be of short duration and have a second order effect on the overall behavior of the instrument.

The rotatory inertia and shear terms are important if the wavelength of the response mode of interest is of the order of the beam thickness. Since the fundamental (first) mode of the system is the one of interest, these terms can be ignored [2].

Note that this is an inherently nonlinear system in that the response frequency is amplitude-dependent. Subharmonic resonance could exist under certain conditions [14]. This is unlikely, however, since the magnitude of the forcing function will be very low ($|\Delta g| \approx 200 \mu\text{gal}$), and stronger motions will be shorter in period and duration and can be filtered from the data.

With instrument applications, it is highly desirable to know what error is introduced by the nonlinearities of the system. In this case, the most conservative method is to compare the static cases of the linear and nonlinear theoretical beams, since both represent opposite extremes of physical practicality. The equation of the nonlinear static beam is

$$EI \frac{\partial^4 y}{\partial x^4} + P_0 \frac{\partial^2 y}{\partial x^2} - \frac{AE}{2L} \frac{\partial^2 y}{\partial x^2} \int_0^L \left(\frac{\partial y}{\partial x} \right)^2 dx + F = 0 \quad (16)$$

and the linear equation is

-
13. B. Carnahan, H.S. Luther and J.O. Wilkes, Applied Numerical Methods, Wiley, New York (1969).
 14. J.J. Stoker, Nonlinear Vibrations in Mechanical and Electrical Systems, Wiley, New York (1950).

$$EI \frac{\partial^4 Y}{\partial x^4} + P_0 \frac{\partial^2 Y}{\partial x^2} + F = 0 . \quad (17)$$

By assuming a deflection curve of

$$Y(x) = \frac{Y_0}{2} \left[1 - \cos \left(\frac{\pi x}{L} \right) \right] \quad (18)$$

and substituting, one obtains

$$F_{NL} = - \left[P_c - P_0 + \frac{AF}{4} \left(\frac{\pi}{L} \right)^2 Y_0^2 \right] \left(\frac{\pi}{L} \right)^2 Y_0 \quad (19)$$

for the nonlinear case, and

$$F_L = - (P_c - P_0) \left(\frac{\pi}{L} \right)^2 Y_0 \quad (20)$$

for the linear case, where P_c is the static buckling load

$$P_c = \frac{EI\pi^2}{L^2} . \quad (21)$$

The percentage of nonlinearity is then

$$\left(\frac{F_L - F_{NL}}{F_L} \right) (100) = \frac{25 AY_0^2}{I(1 - P_0/P_c)} . \quad (22)$$

For design purposes, it is convenient to have a simplified closed-form solution to the general equations in order to establish basic instrument dimensions. This is most easily accomplished by using Rayleigh's Principle [2,3,12].

Applying Rayleigh's Principle yields

$$\omega^2 = \frac{\int_0^L EI \left(\frac{\partial^2 y}{\partial x^2} \right)^2 dx - P \int_0^L \left(\frac{\partial y}{\partial x} \right)^2 dx}{\int_0^L \mu y^2 dx + m y^2 \Big|_{x=L}} , \quad (23)$$

where

$$y = \sum_{n=1}^K a_n \phi_n(x) , \quad (24)$$

ϕ_n are admissible functions which satisfy the geometric boundary conditions, and a_n are constants.

Since each natural frequency of the system is a stationary point,

$$\frac{\partial}{\partial a_n} (\omega^2) = 0 . \quad (25)$$

Although the fundamental mode is the measurement mode, it is important to evaluate unwanted modes. Therefore assume

$$\phi_1(x) = \left[1 - \cos \left(\frac{\pi x}{L} \right) \right] \quad (26)$$

$$\begin{aligned} \phi_2(x) &= \cos \left(\frac{\pi x}{\alpha} \right) - 1 , & 0 \leq x \leq \alpha \\ &= -2 \cos \left[\frac{\pi(x-\alpha)}{L-\alpha} \right] , & \alpha \leq x \leq L \end{aligned} \quad (27)$$

where $\alpha = 0.414L$. The result for the assumed fundamental mode shape is

$$\omega_1 = \left[\frac{EI \left(\frac{\pi}{L} \right)^4 - P \left(\frac{\pi}{L} \right)^2}{\frac{4m}{L} + 3\mu} \right]^{1/2} . \quad (28)$$

As $P \rightarrow P_c$, $\omega \rightarrow 0$, where P_c is the classic buckling load as previously defined. As $P \rightarrow P_c$, the second harmonic

$$\omega_2 \rightarrow 4.3\pi^2 \cdot \left(\frac{EI}{mL^4} \right)^{1/2} , \quad (29)$$

where the assumption was made that the beam mass (ρL) is much smaller than the seismic mass. Theoretically, then, any size beam and seismic mass could be used to obtain the desired system frequency by properly varying the end load.

It should be noted at this point that the fundamental mode shape assumed above (Eq. 26) is correct for $P \rightarrow P_c$ if one examines the linear solution. This means that for high end loads the estimate given for the fundamental frequency in Eq. 28 becomes an accurate guideline in the design of this instrument.

It is now possible to return to the nonlinear equation and observe that the effective seismic mass is the denominator of Eq. 28. The equation for the system including only the nonlinear effect becomes

$$EI \frac{\partial^4 y}{\partial x^4} + P_0 \frac{\partial^2 y}{\partial x^2} - \frac{AE}{2L} \frac{\partial^2 y}{\partial x^2} \int_0^L \left(\frac{\partial y}{\partial x} \right)^2 dx + \mu(x) \frac{\partial^2 y}{\partial t^2} = 0 , \quad (30)$$

where

$$\mu(x) = \begin{cases} \text{mass per unit length for } x < L \\ \frac{m_e}{L} \text{ at } x = L . \end{cases} \quad (31)$$

The boundary conditions are

$$\begin{aligned} y(0,t) &= 0 \\ \frac{\partial y}{\partial x}(0,t) &= 0 \\ \frac{\partial y}{\partial x}(L,t) &= 0 \\ y(L,t) &= y_0(t) . \end{aligned} \quad (32)$$

By assuming the response to be

$$y(x,t) = \frac{y_0(t)}{2} \left[1 - \cos\left(\frac{\pi x}{L}\right) \right] , \quad (33)$$

and evaluating the time response at $x=L$, the result is a Duffing equation:

$$\frac{m_e}{L} \ddot{y}_0 + \frac{AE}{4} \left(\frac{\pi}{L}\right)^4 y_0^3 + (P_c - P_0) \left(\frac{\pi}{L}\right)^2 y_0 = 0 . \quad (34)$$

Assuming small deflection theory about equilibrium ($y_0=0$) results in the natural frequency as a function of end load.

$$\omega_n = \frac{\left[(P_c - P_0) \left(\frac{\pi}{L}\right)^2 \right]^{1/2}}{\frac{m_e}{L}} . \quad (35)$$

By direct comparison,

$$m_e = 4m + 3\mu L . \quad (36)$$

Denoting Eq. 35 as ω_0 , Eq. 34 may now be written in standard form as

$$\ddot{y}_0 + \alpha y_0 + \beta y_0^3 = 0 , \quad (37)$$

where

$$\alpha = \omega_0^2 \quad (38)$$

and

$$\beta = \frac{AEL \left(\frac{\pi}{L}\right)^4}{4m_e} \quad (39)$$

By considering the frequency response of Eq. 37 to a forcing function of amplitude F , the existence of the first subharmonic (subharmonic of order 1/3) depends on the relation [15]

$$\omega_f > 3 \left[\alpha + \frac{21}{1024} \left(\frac{F}{\alpha}\right)^2 \right]^{1/2}, \quad (40)$$

where ω_f is the forcing frequency.

Clearly, Eq. 40 illustrates that subharmonic oscillations could occur for excitation frequencies as low as three times the system's linear natural frequency for very small forces. Therefore, some care must be taken with respect to the frequency content of the locale in which the instrument is placed. (A seismic pier is usually the best location.) It should also be pointed out that larger magnitude excitation at higher frequencies could also occur. Even if this does occur, there will be little concern (other than damage to the elastic members), since strong motions are very short in duration in comparison to the range of interest.

For a vertical gravimeter, the system must measure a variation about mean gravitation on the order of 10^{-9} . As stated above, small deflection theory is assumed to obtain the system fundamental frequency. Therefore an initial compensation must be made for the ambient force of gravitation on the system. This is done by preforming the beam in the fundamental mode shape. Figure 4 shows the effect. K_B is the effective spring constant for a deflection at the mirror holder due to the elasticity of the beam. Y_I is the initial upward deflection, determined so that the force when the system is horizontal just balances the force on the system due to mean gravity ($m_e g_0$). The effect of the end load is a negative spring force K_p . The sum of K_B and K_p is K_E , the effective spring constant actually observed. By varying P and therefore K_p , the desired K_E (and corresponding system frequency) can be obtained.

15. R. Weiss and B. Block, "A Gravimeter to Monitor the $0S_0$ Dilational Mode of the Earth," Journal of Geophysical Research, Vol. 70 (1965) p. 5615.

SYSTEM DESIGN

Electro-Optical

The Fabry-Perot cavity used in this design has a mirror separation of 76.6 cm corresponding to a free spectral range of 195 MHz (Eq. 2). The illuminating laser used for the instrument has a free spectral range of 250 MHz ($L = 60$ cm). This guarantees that there will always be a fringe within the dynamic range of the laser heterodyne system, which is essential for continuous measurements. A flat mirror ($R=\infty$) with a diameter of 7.75 cm (commercially available size) was selected since the spot size W_1 (which is also the beam waist size in this case), is 0.788 mm. The concave mirror diameter was chosen such that it was much larger than its corresponding spot size (1.31 mm) in order to allow enough freedom for adjustment. The radius of curvature chosen for the concave mirror was 120 cm, the next commercially available size larger than the mirror separation distance. (Half concentric systems are stable for $R>L$ [7].) Mirrors with a reflectivity of 0.99 were selected, resulting in a theoretical finesse of 300 (Eq. 4). The full width at half maximum is then 2 MHz (Eq. 3).

The laser heterodyne system was adapted from a previous experiment [16] and is essentially the design of J. Levine and J.L. Hall [1]. The illuminating laser is a nonconfocal system (mirror radii do not share a common center of curvature) with a beam waist, W_0 , of radius 0.71 mm. The beam waist is located 48 cm from mirror 1 (Figure 1). With this information, using a mirror with a radius of 120 cm (stock size and satisfying the focal length requirement of $f>f_0$ (Eqs. 6-8)), mode matching was accomplished using the parameter $d_1 = 85$ cm and $d_2 = 31$ cm. The servosystem of the illuminating laser has been designed for a resolution of one part in one thousand when locked at the peak of a fringe. This corresponds to an uncertainty of 2 kHz or a 0.05-Å detection capability. On this basis, 1-Å resolution was assumed as a conservative parameter for the actual retro-reflector design.

The Fabry-Perot cavity is constructed from fused quartz and mild steel (Figures 5 and 6). The effect of temperature on the cavity length is compensated for by the re-entry of the steel retro-reflector support into the cavity which is supported on quartz rods (Figure 6). The relative dimensions of steel and quartz were designed according to their respective thermal expansion coefficients. In order to maintain an all quartz configuration elsewhere, the upper mirror is set upon a small glass disk which is free to slide within a larger spherical face cut into a quartz disk (Figure 7). This disk can be mounted with the concave side either up or down, and is clamped as illustrated in Figure 6.

The methane stabilized laser (Figure 8) is a HeNe laser with a methane cell mounted within the laser cavity. One mirror is mounted on a piezoelectric element, and the other is permanently fixed. A small ac dither voltage and a variable dc voltage are impressed on the piezoelectric element.

-
16. E.F. Homuth, "The Comparison of Fused Quartz Earth Strainmeters with a Methane Stabilized Michelson Interferometer Earth Strainmeter," Ph.D. Thesis, Geophysics, University of Washington, 1974.

The light transmitted through the methane absorption cell is photoelectrically detected. The resultant signal is amplified and synchronously detected, by using the dither frequency as a reference. The digital servosystem [16] uses a combination of NAND gates and edge triggered flip-flops to produce two error pulses per cycle of the signal. The duration of the error pulse is proportional to the phase difference between the reference signal and the laser output signal. The error pulses are then integrated and applied to the piezoelectric element driver. This servoloop locks the methane laser frequency to the peak of the absorption line in methane. The characteristics of this system have been previously established [16]. The width of the methane peak at half maximum is about 200 kHz. The digital servolock is capable of locking to within 1/100 of this peak, resulting in a stability of 2 parts in 10^{11} which corresponds to an uncertainty of ± 2 kHz.

A preliminary check on the overall stability of the methane stabilized laser has been reported by Levine and Hall, who computed the Allen variance of two independently stabilized methane lasers by measuring the average fluctuation of the heterodyne frequency, as a function of the averaging time [1]. The Allen variance is expressed as the ratio of these quantities to the output frequency (approximately 10^{14} Hz). For sampling intervals longer than 10 seconds, the Allen variance is on the order of 10^{-13} , or less. Therefore the assumption of 2 kHz is conservative.

The operation of the long path phase lock is basically identical to that of the methane stabilized laser, except that the methane cell has been removed and the fringes of the Fabry-Perot cavity are followed instead of the methane line. The servosystem in this case is an analog design identical to the type used by Levine and Hall [1]. As described above, the overall system results in an uncertainty of ± 2 kHz. An added feature of this system is the passband filter stage for improving the input signal-to-noise ratio from the detector.

A modification to the Levine-Hall design allows automatic shifting when the laser approaches its dynamic limits. The dynamic range of the long path laser is limited because of the emission of two light frequencies simultaneously at the extremes of the Doppler profile [7,16]. This provides for a completely automated system which requires little attention during operation, as well as a linear dynamic range limited only by the geometric nonlinearities of the mechanical system.

Mechanical

Considering the retro-reflector system (see Figures 5 and 6), and assuming the 1-Å deflection (Z_{\min}) sensitivity discussed above, the desired natural frequency, f_n , can be computed as

$$f_n = \frac{1}{2\pi} \left(\frac{\Delta g_{\min}}{Z_{\min}} \right)^{1/2} \text{ Hz} , \quad (41)$$

where Δg_{\min} , the desired resolution of changes in gravity, is in the microgal region (10^{-6} cm/sec²). Therefore the required frequency in the detection (fundamental) mode is on the order of 2 Hz.

Since the mirror holder (seismic mass) is the smallest component, a size compatible with standard mirror sizes was selected. The mirror holder was designed such that the center of mass, mirror face, and beam neutral plane were all coincident. Failure to do so would result in spurious signals due to momentary misalignments caused by excitation of unwanted modes. Connection to the beam is provided by a flange joint where the beam and mirror holder are machined to be self-centering. The mirror is held against the neutral plane of the beam, and its dimensional integrity maintained by inserting a rubber O-ring between the mirror and the lower clamping member. To maintain a controlled boundary condition at the seismic mass and provide a gauge surface for beam length comparisons, flat surfaces perpendicular to the beam were machined from the mirror holder where the beam protrudes. The computed mass of the mirror, mirror holder, screws, and the portion of beam clamped by the holder is 110.4 gm. The mirror holder is 3.0 cm in diameter and 2.09 cm high when assembled.

A rectangular beam shape was chosen such that beam stresses (corresponding to a reduced natural frequency of 1 Hz (Eq. 2b) were low in comparison to the ultimate yield strength of high-strength spring steel. The resulting system was then checked for adequate mode separation at the reduced fundamental frequency. The final beam dimensions were

$$\begin{aligned}L &= 5.08 \text{ cm} \\W &= 0.67 \text{ cm} \\t &= 0.067 \text{ cm.}\end{aligned}$$

The critical buckling load for the above system is 14.2×10^6 dynes. The end load to obtain a natural frequency of 2.5 Hz is 13×10^5 dynes. When the fundamental frequency is 2.5 Hz, the next highest symmetric bending mode is 200 Hz and therefore well separated. Other modes are also possible. The rotational mode about a horizontal axis perpendicular to the beam axis is sufficiently separated at 114 Hz. The end load has a negligible effect on this frequency for small oscillations. The torsional mode about an axis along the beam axis is 73 Hz and is also unaffected by end load. The design stresses are far below the yield or cold creep stress levels [17] of the spring steel material used (1.38×10^{10} dynes/cm²).

Constant boundary conditions (zero end slope) are maintained during loading by a parallel flexure support system (Figure 5). The flexure used was a rectangular cross section beam with a semicircular section removed. The resulting flexure has a linear relationship between the applied moment and the angle of rotation of one end of the section relative to the other. A motion parallel to the base and neutral plane of the beam was obtained.

17. J.D. Lubahn and R.P. Felgar, Plasticity and Creep of Metals, Wiley, New York (1961).

The massive frame as shown in Figure 6 was designed with a large safety factor to ensure maximum rigidity. A simple lever and weights end-load the beam (15 to 1 ratio). Once the required loading is determined and applied, the parallel motion supports are clamped securely with clamp blocks and screws mounted transverse to the supports, assuring minimum instrument drift. (Drift here means a loss of sensitivity and calibration.) Taper pins are used to transmit shear and align the assembly during construction. Bolts are used to transmit moments and shear to the cross members. All four sections are 3.175 cm thick and were made from mild steel for machinability. The frame can be considered rigid relative to beam compression loads. Two additional sides could also be added to shield the sensing element from magnetic influences.

SYSTEM OPERATION

Optical Alignment

Optical alignment of this system is not a trivial operation, primarily because 3.39μ light is in the far infrared spectrum and invisible not only to the naked eye, but to all commercial viewers and infrared phosphorescent materials. Therefore, initially one must use a visible source for boresighting the optical equipment. The procedure used was to set the system up roughly in the desired position so that a 6328-\AA (visible red) source could freely pass throughout the lasers, cavity, and beam splitter (Figure 8). Then, by removing mirror number 2 and inserting suitable optics, the 3.39μ path source was directed a convenient distance and detected with a photodiode. Maximizing the output signal from the detector ensured that the diode was in the center of the invisible light beam (Gaussian intensity distribution [7]). With the 3.39μ laser turned off, the visible red source was adjusted so that the detector output signal was again maximized. This results in the visible light beam being collinear with the infrared source. This procedure was repeated with the methane laser by removing the photodiode. Alignment of the methane laser is for the purpose of superimposing the beams of the two infrared lasers on the interference frequency diode to obtain a heterodyne frequency.

The mirrors used in the Fabry-Perot cavity transmit 1% at 3.39μ , and for all practical purposes are opaque to visible red light. However, by placing a pin hole at the exit of the long path source, and removing the retro-reflector assembly, the visible light is reflected back to the pin hole from the fixed mirror. The same procedure is followed for the retro-reflector. With the infrared lasers on, interference fringes can be detected by placing the photodiode (Figure 8) behind the fixed mirror, and dithering the long path laser over a half wavelength. Both mirrors are then adjusted for a maximum signal-to-noise ratio fundamental fringe, and minimum higher order (off-axis) optical modes [1,7].

Mechanical Alignment

The mechanical system can be tuned by clamping one end of the beam and loading or unloading the other end of the beam to develop the desired natural frequency. The present design can be tuned from 2.5 Hz to 21.6 Hz. This corresponds to four orders of magnitude in sensitivity adjustments which

will allow for accurate measurements of earthquakes, microseisms, teleseisms, and earth tides, depending on the sensitivity required and the magnitudes of the ground motions of interest. Deformation due to loading may require small readjustments in the optical alignment of the retro-reflector, but fringes will still be detectable, unless beam buckling has occurred.

Data Acquisition

The overall system sensitivity is determined by the square of the fundamental frequency multiplied by the optical system sensitivity. For the 2.5-Hz (15.7 rad/sec) natural frequency, and 1-Å optical resolution, the system sensitivity is 2.46 μgal and the required sensitivity is attained. The change in heterodyne frequency per microgal is 5.3 Hz (from Eq. 1).

The heterodyne frequency detected is monitored by a frequency counter with a high-stability time base and binary-coded decimal output options. For this work, the output was recorded as an analog signal on a strip chart recorder by using a digital-to-analog converter. In its final form, the BCD output would be recorded directly on tape for future data reduction.

RESULTS

Mechanical System

Preliminary frequency tests were accomplished by using a stroboscope and exciting the mass by tapping it with a small rubber mallet. This method is preferable to magnetic excitation since such an exciter could leave a permanent magnetic field in the beam and structure that would change with time. Frequency tests with the beam clamped, but with flexure supports not bolted to the frame, gave a natural frequency of 21.6 Hz as opposed to 13.6 Hz when the supports were bolted. This was interpreted as an overall tolerance error in the construction of the mechanical system. This error was expected since an overall error of 0.05 cm in the compressive direction would result in buckling of the beam.

The natural frequency reduction obtained with both ends clamped was 71.9%, corresponding to a reduced frequency of 6.1 Hz (Figure 9).

Another possible loading method is to clamp one end, leaving the second end unclamped and loaded to the desired natural frequency. This method yielded 2.5 Hz, a frequency reduction of 88%, and is within the range of interest. (Leaving the weights, tray and loading lever in the "load" position has a second order effect.) It should also be pointed out that this procedure reduces the effect of geometric nonlinearity since the change in beam strain is reduced (Eq. 11).

Electro-optical System

The usable range of heterodyne frequencies of the laser system is between -70 MHz and 125 MHz. This was measured by sweeping the piezoelectric element with a dc voltage while keeping the methane stabilized laser locked on the methane absorption line. The asymmetry of the range is due to relative gas pressures of the methane cell and helium-neon gain cell. That is, the methane line is not centered at the top of the Doppler profile of the helium-neon gain cell (Figure 10).

The radio frequency transmitter used to pump the lasers is operated at 150 MHz, so extensive shielding of the beat frequency detection and readout system was necessary. Positioning the readout system for a minimum RF level, and tuning the transmitter and lasers for a maximum signal output and minimum reflected (and radiated) signal, is also necessary in order to obtain a clean heterodyne frequency that does not include the unwanted 150 MHz.

The final system configuration illuminates the Fabry-Perot cavity through the retro-reflector, and detects the fringes by mounting the detector on top of the structure. One difficulty with this arrangement did become apparent. The fringes were steady in frequency (i.e., the seismic mass was not responding in unwanted, higher mechanical frequency modes), but they did vary in intensity. This was observed by dithering the illuminating laser frequency over a wide band (frequency modulating the light), and observing the transmission fringes of the cavity on an oscilloscope triggered by the dither signal. Translations of the seismic mass appear as fringe translations along the time axis, whereas intensity variations (which should not exist) appear as changes in peak voltages on the vertical axis. The variation in intensity was a result of structural sway of the cavity, causing the focused light on the photodiode of the detector to wander over the diode surface. The servosystem interprets a change in intensity as a light frequency error, and responds by changing the dc voltage on the piezoelectric element, which results in an increased, rather than decreased, error signal. Thus, except for very low loop gain, the servosystem would become unstable. This problem was corrected by stiffening the structure with cross members between the quartz rods such that changes in the length of the cross members due to temperature fluctuations were independent of the stiffening members (Figure 11).

The long path servosystem requires about 1-1/2 msec to make a correction to a step input. This corresponds to a bandwidth of well over 100 Hz. The dc loop gain of 120 dB yields negligible static errors.

Overall System Performance

To prove conclusively that the system has microgal resolution would require data collection over a period of several months from a quiet site, such as a seismic pier. However, for checkout purposes, the system was set up in the basement of the Applied Physics Laboratory at the University of Washington. A granite slab was set on several concrete blocks which in turn rested on the basement floor. All of the optical components, as well as the

Fabry-Perot cavity, were then mounted on the granite slab. The entire apparatus was surrounded by a polyethylene tent to reduce air convection and dust contamination. The Fabry-Perot cavity was not surrounded by an evacuated container, which would make adjustments to the system time consuming at this stage of development. (An evacuated container is required for field evaluations, however.)

One can qualitatively demonstrate resolution on the order of 1 μgal if the required natural frequency of the mechanical system is known, and the recorded variance of averaged samples corresponds to the required optical sensitivity of the instrument. Since the sensitivity of the mechanical system has been shown to be 2.46 $\mu\text{gal}/\text{\AA}$, it is necessary to demonstrate an optical resolution of 0.4 \AA . In order to determine the extent of optical resolution, it was necessary to raise the natural frequency of the mechanical system to 39.5 Hz. This was necessary because ambient noise made it impossible for the servo system to follow seismic mass deflections at higher sensitivities. At the reduced sensitivity, it was then necessary to shut down the elevators after normal business hours in order to record relatively quiet data.

A sample record is shown in Figure 12. A full-scale reading on the strip chart corresponds to a heterodyne frequency of 10 MHz. The frequency counter used in this experiment was set to sample and average the system response over a period of 1 second. The large deviations of 1 MHz were due to personnel moving around the apparatus (about 5 meters away from the cavity). The quiet zones in the record occurred when the building was acoustically quiet. The variations in the record during quiet periods appear to be approximately 200 kHz, which corresponds to a deflection resolution of 15.4 \AA . This is an upper bound on the optical resolution, since it still includes variance in ground motion, air pressure, and air temperature.

The mechanical sensitivity at the beam natural frequency of 39.5 Hz is 615 $\mu\text{gal}/\text{\AA}$. The theoretical sensitivity of the optical system is 0.077 $\text{\AA}/\text{kHz}$. The 1-MHz peak disturbance apparent in the record shown in Figure 12 represents a 47.4 mgal building disturbance. Disturbances as large as 0.3 gal have been observed during the day, making accurate measurements difficult.

In view of the high resolution of the optical system under such adverse conditions, it is highly probable that the required instrument sensitivity has been obtained, and that the instrument is ready for a field evaluation in an evacuated container on a seismic pier.

CONCLUSIONS AND RECOMMENDATIONS

A methane absorption stabilized laser system and seismic sensor system using an endloaded beam suspension for variable sensitivity (frequency) have been combined in a gravimeter design. The resolution of the laser system is in the range of 1 \AA . The natural frequency of the seismic system as presently operated is 2.5 Hz, which allows microgal resolution. Although some drift is apparent in the present records, it is believed that adequate isolation in an evacuated container will reduce the drift error to negligible proportions over long periods.

It is apparent that such a short-term evaluation of instrument performance with an instrument designed to record over long periods of time is not truly conclusive evidence of the good performance of the instrument. Therefore, it is highly recommended that an evaluation take place over several months at a quiet seismic pier. Such a study might reveal design faults that are not discernible in the records of the seismically noisy zone presented here.

A preliminary study of the response of an accelerometer with time-varying spring stiffness has been conducted. This type of parametric excitation has produced a substantial increase in the gain of a seismometer using a varying magnetic field for a suspension system [18]. The end load of the present design may be varied sinusoidally by an appropriate transducer, and, in fact, endloading may momentarily be raised above the buckling load by this excitation without buckling, since a finite time is required for buckling to occur. It is believed that this improvement may very well take the sensitivity of gravimeters into a new realm, since preliminary experiments by Rogers have yielded an increase in gain of three orders of magnitude [18].

It is now possible to build a laser heterodyne system using visible red (6328 Å) light, by locking on to the hyperfine component in iodine rather than the (previously state-of-the-art) methane absorption line using 3.39 μ infrared radiation [19]. It is believed that a conversion to the visible red portion of the spectrum should be seriously considered for this system. Such a conversion would allow the system to be reduced by almost one-fifth of its present size (cavity) and alignment would be greatly simplified with visible light. Furthermore, such a system might be pumped by a dc voltage, rather than RF-excited as in the present system, therefore eliminating the shielding difficulties experienced with the present system.

-
18. P.W. Rogers, "A Phase Sensitive Parametric Seismometer," Bulletin of the Seismological Society of America, Vol. 56, No. 4 (August 1966) pp. 947-959.
 19. G.R. Hanes, K.M. Baird and J. DeRemigis, "Stability, Reproducibility, and Absolute Wavelength of a 633-nm He-Ne Laser Stabilized to an Iodine Hyperfine Component," Applied Optics, Vol. 12, No. 7 (July 1973) pp. 1600-1605.

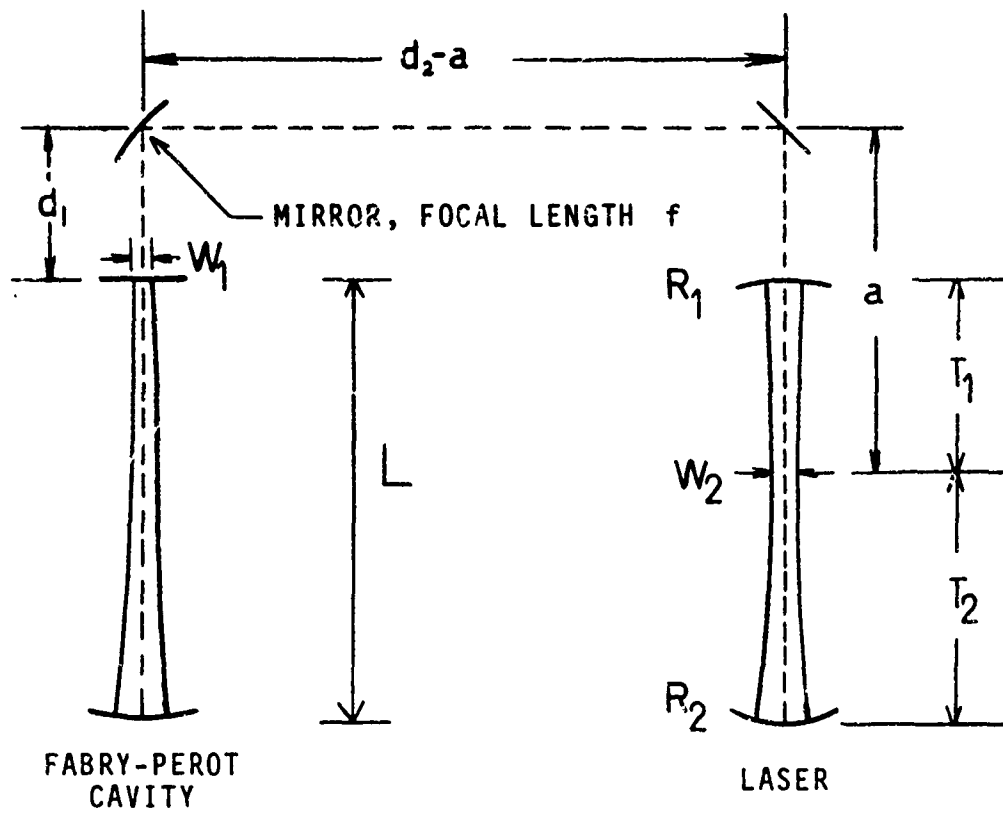


Figure 1. Cavity-laser system

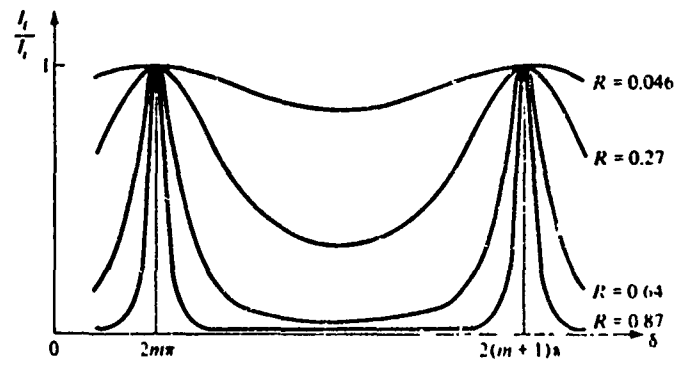


Figure 2. Transmission characteristics of a Fabry-Perot etalon [7]

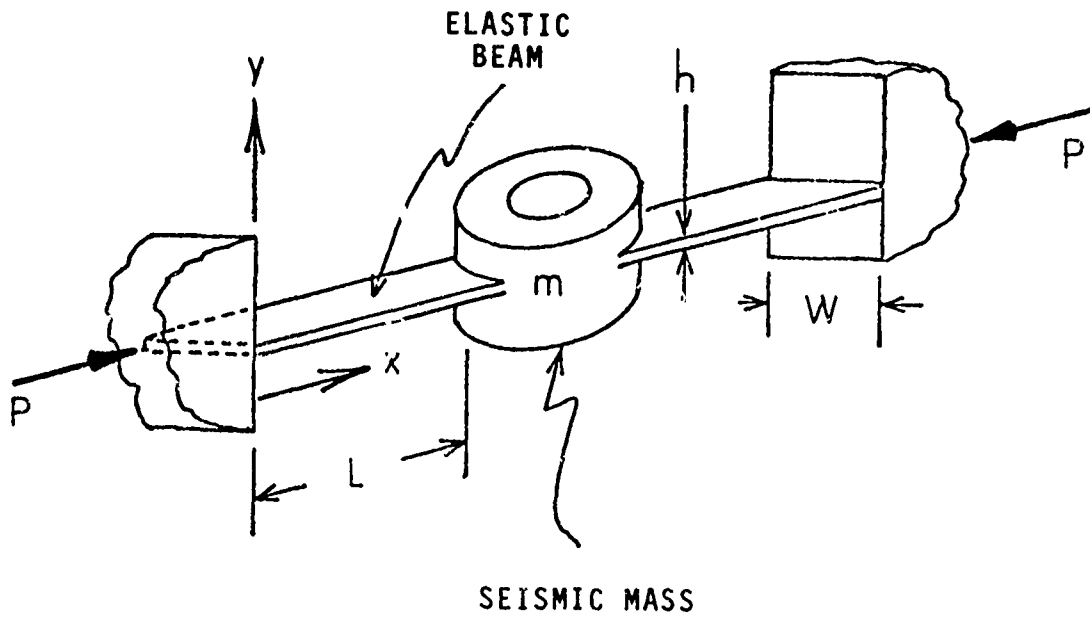


Figure 3. Retro-reflector suspension

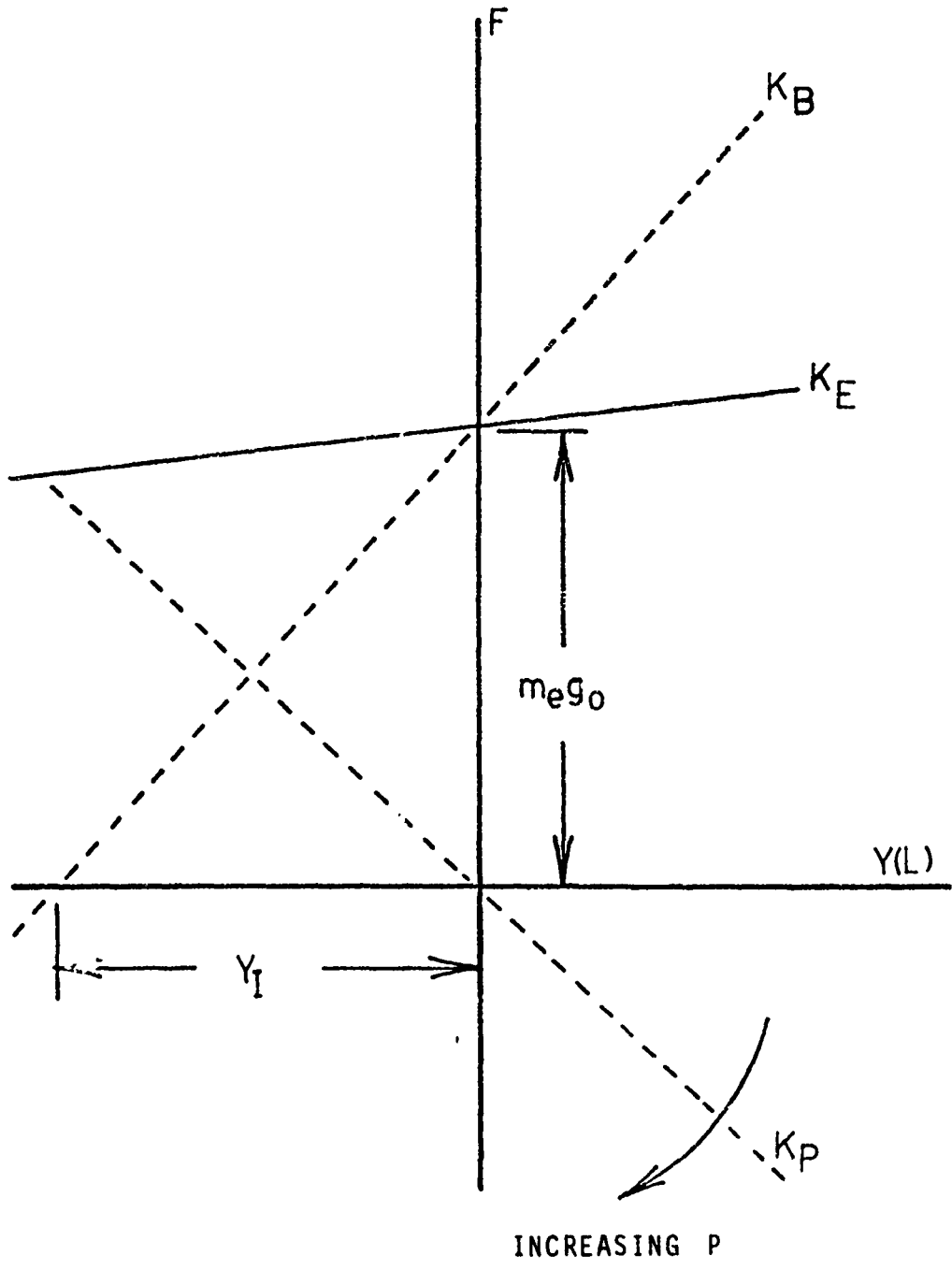


Figure 4. Gravitational compensation

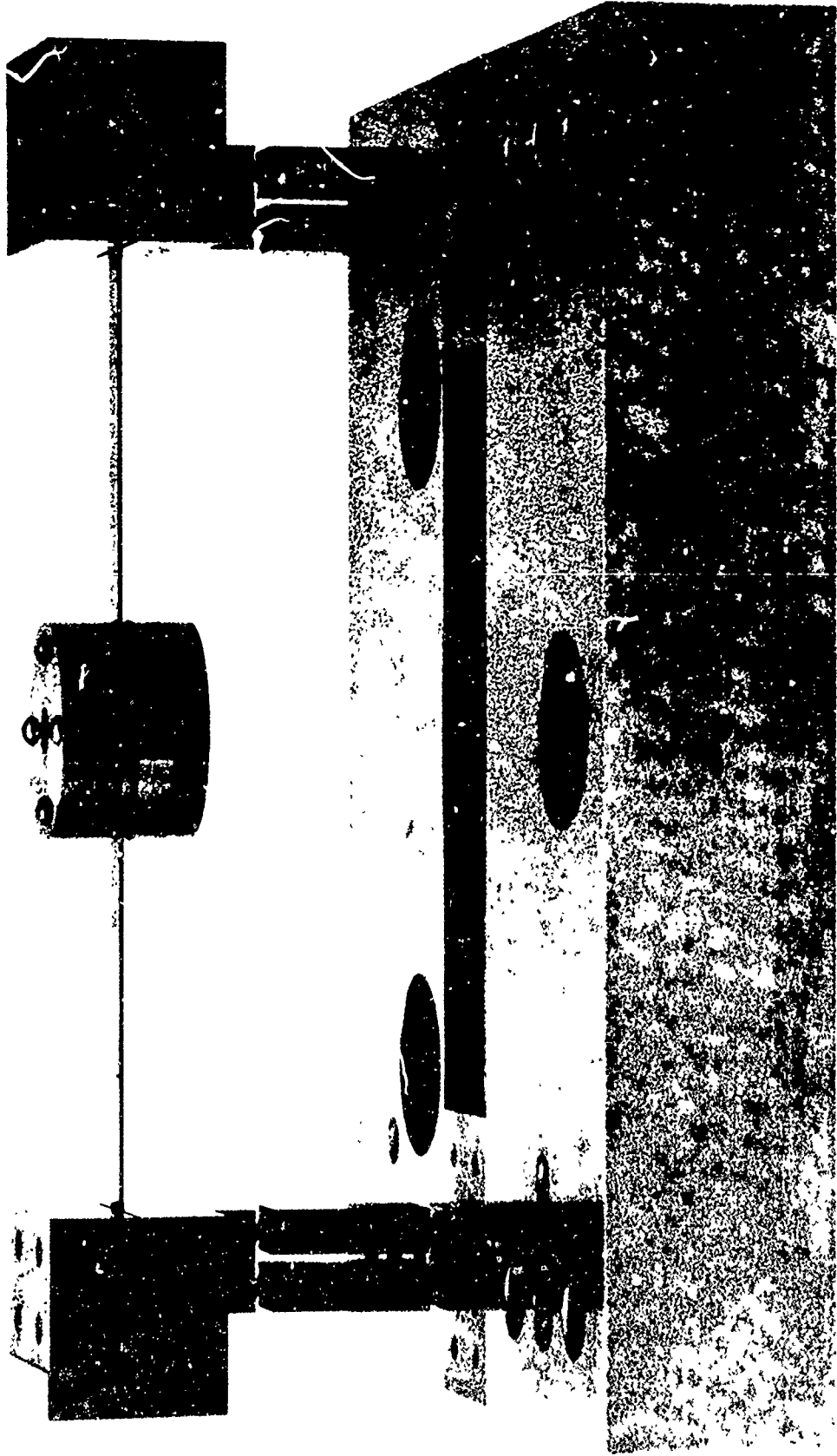
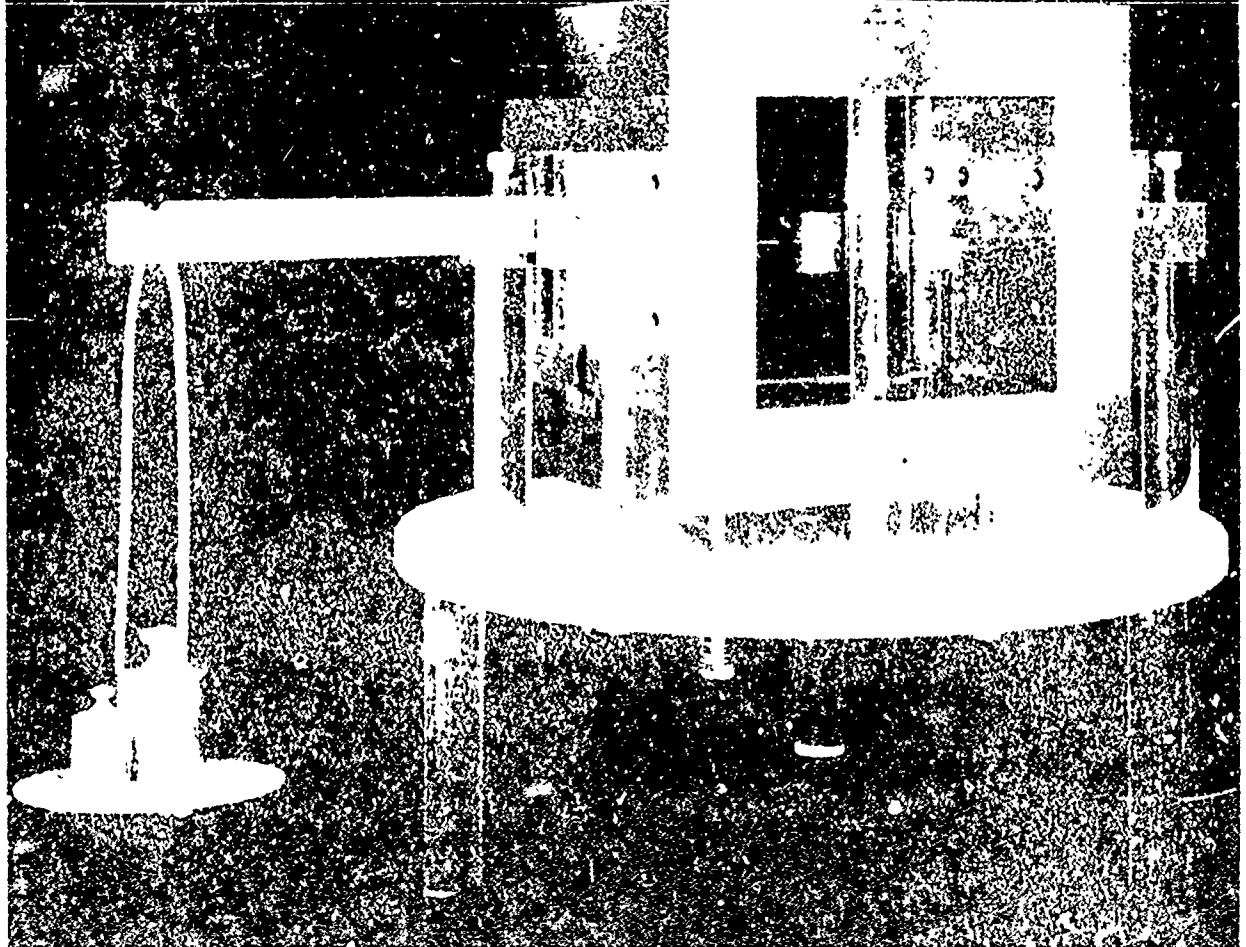
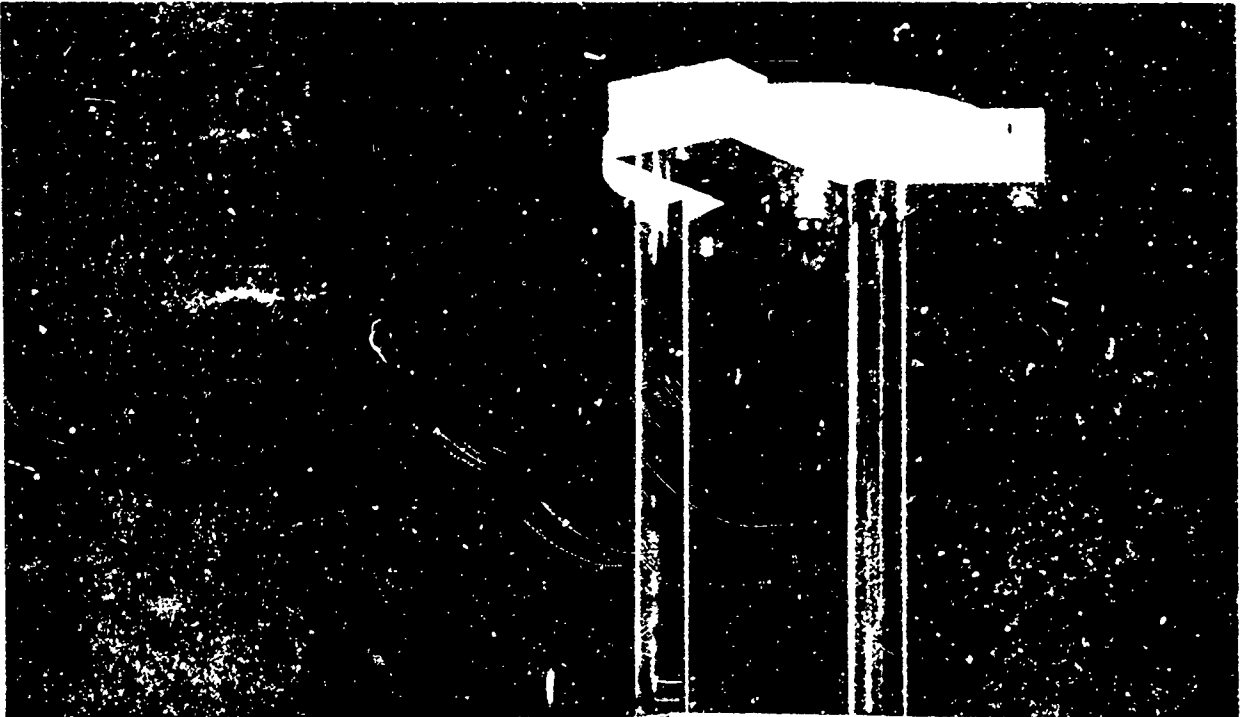


Figure 5. Retro-reflector subassembly



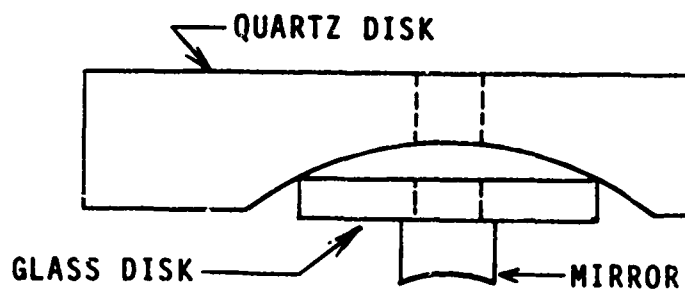


Figure 7. Upper mirror assembly

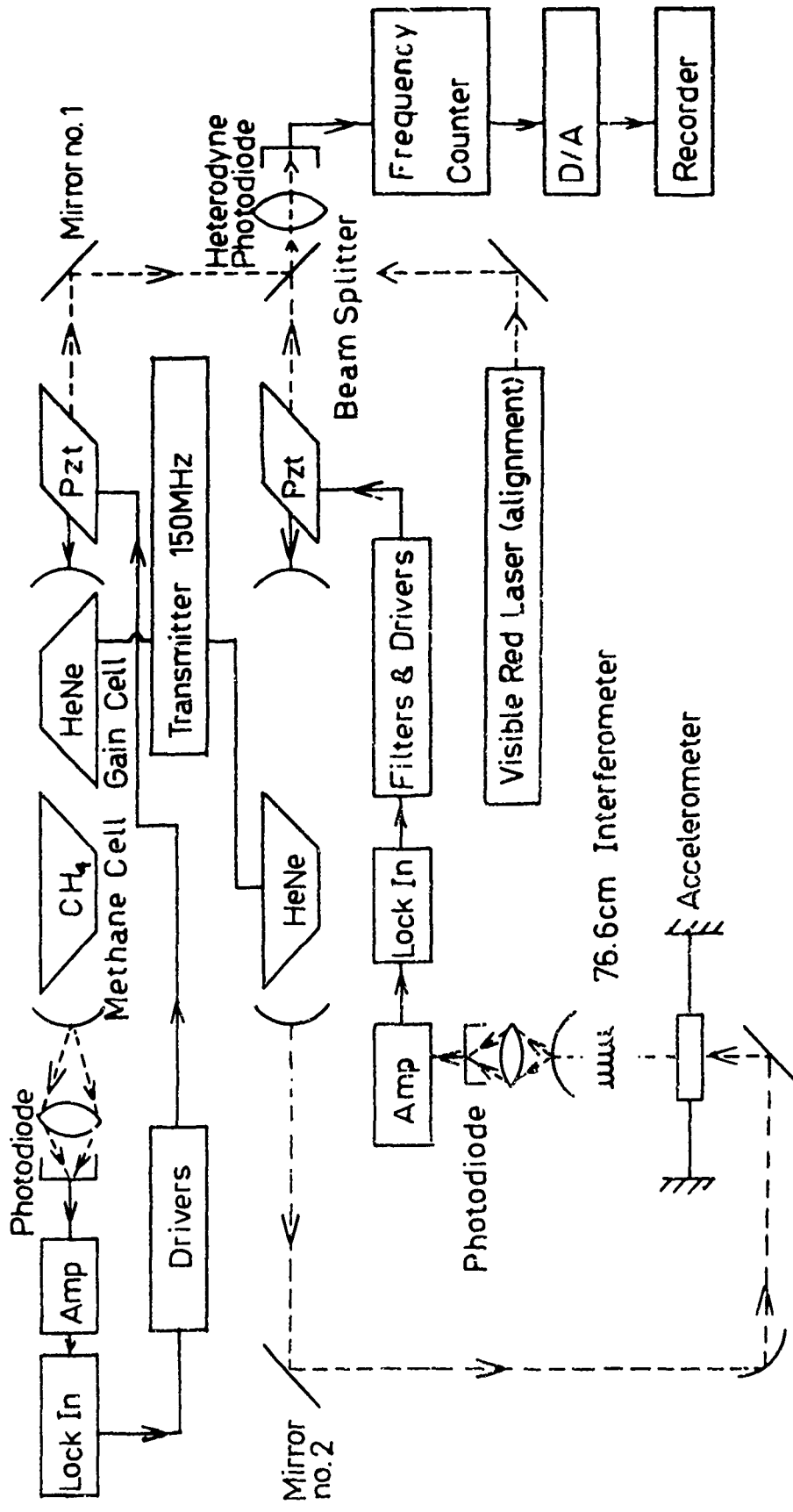


Figure 8. System schematic

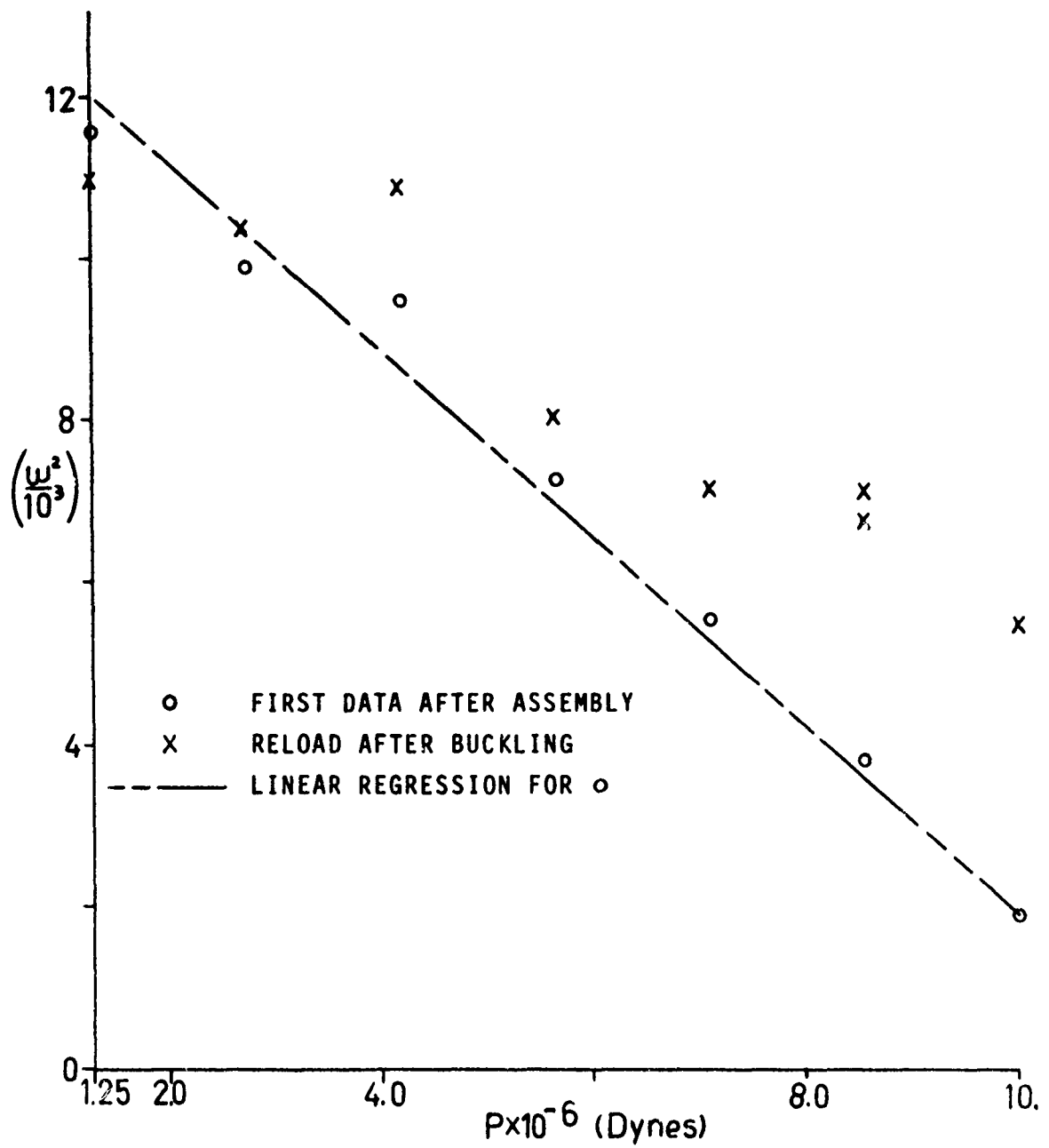


Figure 9. Frequency vs end load

LASER POWER
INTENSITY

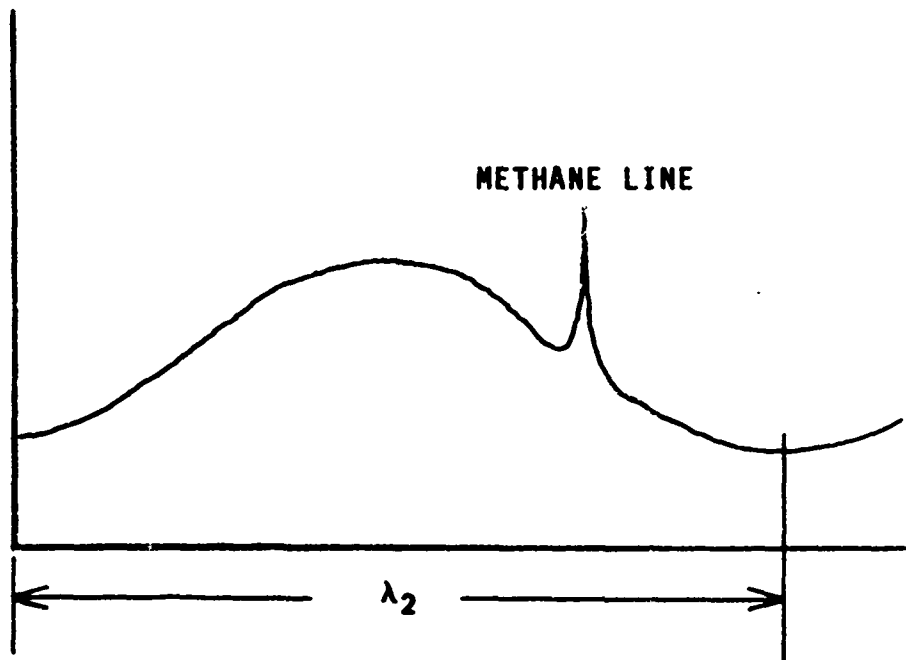


Figure 10. Asymmetry of the methane line

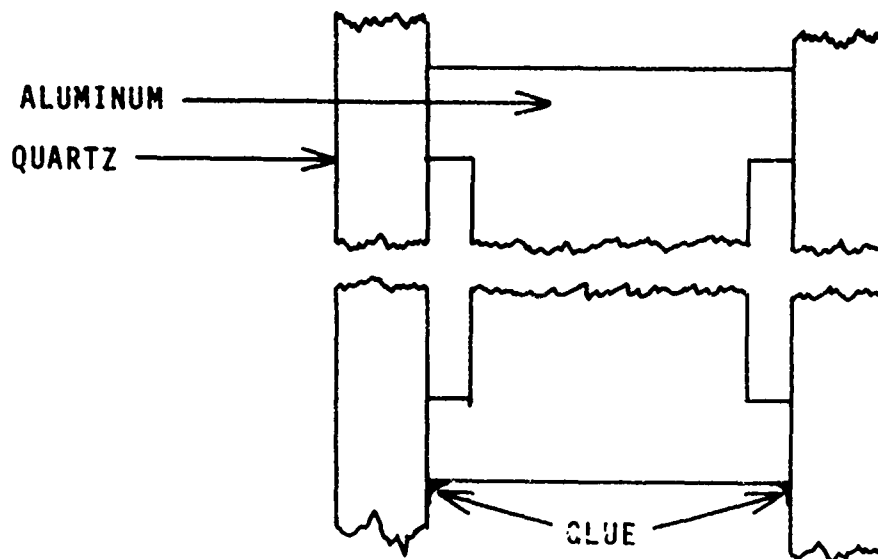


Figure 11. Structural stiffener

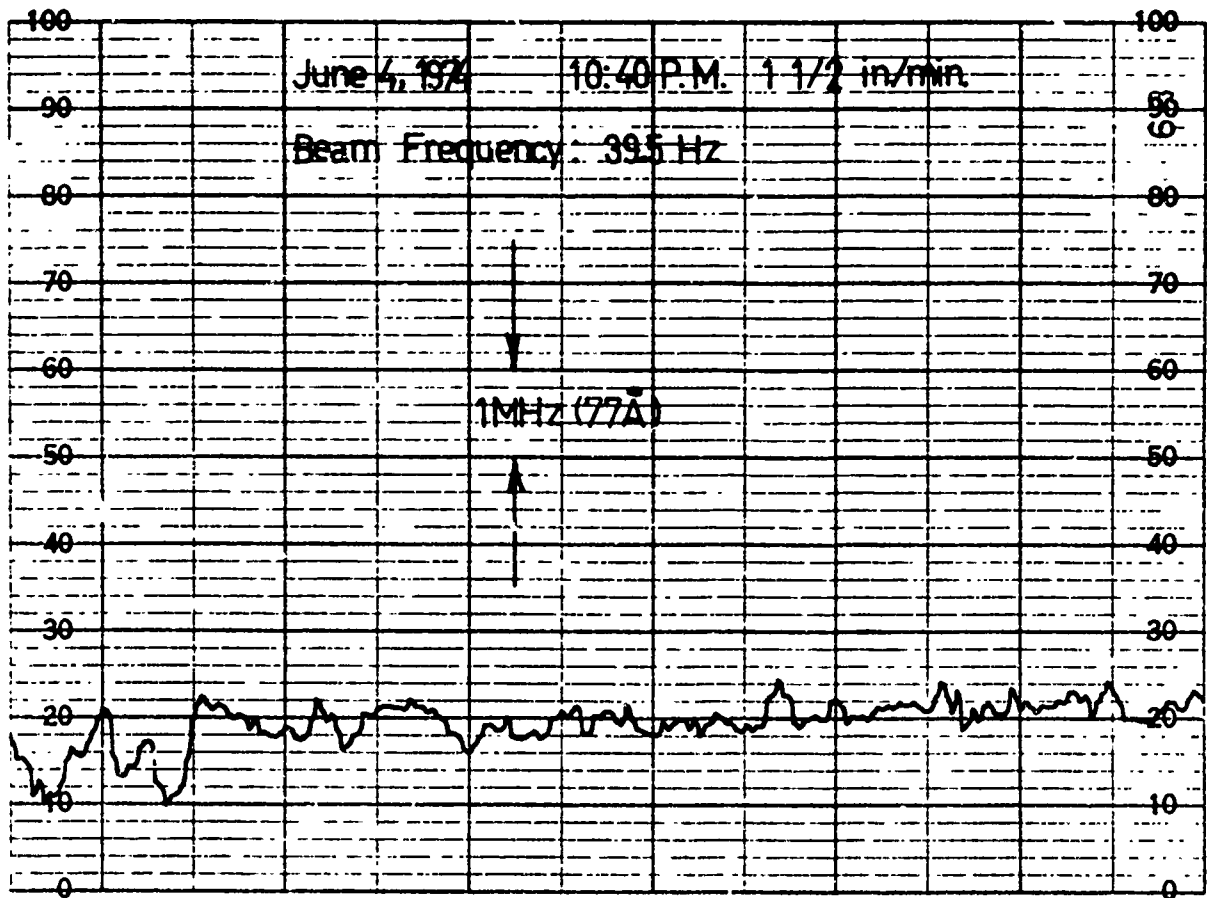


Figure 12. Ground motion record

REFERENCES

1. J. Levine and J.L. Hall, "Design and Operat.on of a Methane Absorption Stabilized Laser Strainmeter," Journal of Geophysical Research, Vol. 77, No. 14 (May 1972) pp. 2595-2609.
2. L. Meirovitch, Analytical Methods in Vibrations, Macmillan, New York (1967).
3. D. Burgreen, "Free Vibrations of a Pin-Ended Column with Constant Distance Between Pin Ends," Journal of Applied Mechanics, June 1951, pp. 135-139.
4. H. Lurie, "Lateral Vibrations as Related to Structural Stability," Journal of Applied Physics, June 1952, pp. 195-204.
5. W.R. Bennett, Jr., "Hole Burning Effects in a HeNe Optical Laser," Physics Review, Vol. 126 (1962) p. 530.
6. W.R. Bennett, Jr., "Hole Burning Effects in Gas Lasers with Saturable Absorbers," Comments on Atomic Molecular Physics, Vol. 2 (1970) p. 10.
7. A. Yariv, Introduction to Optical Electronics, Holt, Rinehart and Winston, New York (1971).
8. H. Kogelnik and T. Li, "Laser Beams and Resonators," Applied Optics, Vol. 5, No. 10 (October 1966) pp. 1550-1567.
9. N.D. McMullen, "Methane Absorption Stabilized Laser Gravimeter: Design of an Ultra-Sensitive Fabry-Perot Interferometer Accelerometer," M.S. Thesis, Mechanical Engineering, University of Washington, 1974.
10. M.A. Southwell, Translated from Russian by M.G. Yatsua, "On the Correction for Shear of the Differential Equation for Transverse Vibrations of Prismatic Bars," Philosophical Magazine, Vol. 41 (May 1921) pp. 288-290.
11. J.C. Snowdon, "Transverse Vibration of Beams with Internal Damping, Rotary Inertia, and Shear," Journal of the Acoustical Society of America, Vol. 35, No. 12 (December 1963) pp. 1997-2006.
12. S. Timoshenko, Vibration Problems in Engineering, VanNostrand, New York (1955).
13. B. Carnahan, H.S. Luther and J.O. Wilkes, Applied Numerical Methods, Wiley, New York (1969).
14. J.J. Stoker, Nonlinear Vibrations in Mechanical and Electrical Systems, Wiley, New York (1950).
15. R. Weiss and B. Block, "A Gravimeter to Monitor the $0S_0$ Dilational Mode of the Earth," Journal of Geophysical Research, Vol. 70 (1965) p. 5615.

16. E.F. Homuth, "The Comparison of Fused Quartz Earth Strainmeters with a Methane Stabilized Michelson Interferometer Earth Strainmeter," Ph.D. Thesis, Geophysics, University of Washington, 1974.
17. J.D. Lubahn and R.P. Felgar, Plasticity and Creep of Metals, Wiley, New York (1961).
18. P.W. Rogers, "A Phase Sensitive Parametric Seismometer," Bulletin of the Seismological Society of America, Vol. 56, No. 4 (August 1966) pp. 947-959.
19. G.R. Hanes, K.M. Baird and J. DeRemigis, "Stability, Reproducibility, and Absolute Wavelength of a 633-nm He-Ne Laser Stabilized to an Iodine Hyperfine Component," Applied Optics, Vol. 12, No. 7 (July 1973) pp. 1600-1605.